WCAP-16996-P, "Realistic LOCA Evaluation Methodology Applied to the Full Spectrum of Break Sizes (FULL SPECTRUM LOCA Methodology)" Requests for Additional Information – Second Set (Non-Proprietary)

May 2013

Westinghouse Electric Company LLC
1000 Westinghouse Drive
Cranberry Township, PA 16066

Question 20: ^{235}U, ^{238}U, and ^{239}Pu Decay Heat Uncertainty Fits to ANS 5.1-1979

Decay heat is an important factor in the analysis of postulated LOCAs and ECCS performance evaluation and an accurate assessment of both the decay heat and its uncertainty is necessary. WCAP-16996-P/WCAP-16996-NP, Volumes I, II and III, Revision 0, Section 9.2, "Decay Heat Source," explains that WCOBRA/TRAC-TF2 solves the time-dependent decay activity differential equation accounting for ^{235}U thermal, ^{239}Pu thermal, and ^{238}U fast fissions. The energy yield constants are weighted by the appropriate fission rate fractions as a function of initial enrichment and burnup within WCOBRA/TRAC-TF2. Section 9.2 states that the WCOBRA/TRAC-TF2 decay heat model was benchmarked against the ANSI/ANS 5.1-1979 Standard. Results of decay heat for ^{235}U computed by WCOBRA/TRAC-TF2 and using the American Nuclear Standards Institute (ANSI)/ANS 5.1-1979 Standard are presented in Table 9-2, which shows that the difference between the values calculated from both approaches is negligible for decay time up to 10^3 s. The section also states that similar comparisons exist for ^{239}Pu and ^{238}U.

The decay heat uncertainty modeling in WCOBRA/TRAC-TF2 is discussed in WCAP-16996-P/WCAP-16996-NP, Volumes I, II and III, Revision 0, Section 9.7, "Decay Heat Uncertainty Evaluation," which explains that WCOBRA/TRAC-TF2 models decay heat uncertainty through the use of pseudo-isotope energy yield augmentation factors generated using a least squares fit to the uncertainty data provided in ANSI/ANS 5.1-1979. The section claims that the results, as provided in Table 9-14, "provide a conservative representation of the standard's quoted uncertainties." Although Table 9-14 presents the computed factors, a description of the uncertainty modeling equations and their implementation in WCOBRA/TRAC-TF2 is not provided. Please provide the equations used in WCOBRA/TRAC-TF2 to compute the decay heat uncertainties for the considered isotopes and explain how the individual uncertainties are used in predicting the overall decay heat uncertainty in plant analyses.

Response:

Equation 9-2 of WCAP-16996-P Revision 0 is solved by WCOBRA/TRAC-TF2 to determine the time dependent decay heat power for a given pseudo-isotope. This equation is as follows:

$$\frac{d}{dt}DH^i = \alpha_i(\Sigma_F\phi) - \Gamma_i DH^i \qquad (1)$$

In WCOBRA/TRAC-TF2, the decay heat uncertainty is modeled by [

]^{a,c} The total decay heat uncertainty is dependent upon the cumulative uncertainty contributions due to each of the pseudo-nuclides. Their relative contributions will

change with burnup and, to a lesser extent, enrichment since the fission fractions of the fissile isotopes (the w_n factors in equation 9-3 of Section 9.2) will change as function of burnup and enrichment.

ANSI/ANS 5.1-1979 requires accounting for the uncertainty in the energy per fission. This uncertainty, which has been determined in WCOBRA/TRAC-TF2 using uncertainty data from ENDF/B-V, is convoluted with the decay heat uncertainty. The uncertainty in the prompt energy per fission is a function of the channel burnup and enrichment since the fission fractions for each of the fissionable isotopes is a function of these variables. Table RAI-20-1 below provides the fitting data for κ and the one sigma uncertainty in κ, σ_κ. Both κ and σ_κ are fitted as functions of burnup, enrichment, and H/U ratio.

Section 9.7 of WCAP-16996-P Revision 0 explains that the A_i terms in equation (2) were determined through a least squares fit of the uncertainty data in ANSI/ANS 5.1-1979. Effectively, these A_i terms reproduce, to a high degree of accuracy, the ANSI/ANS 5.1-1979 decay power with 2σ uncertainty over the range of cooling times given in Tables 4-6 of ANSI/ANS 5.1-1979 for the three fissionable isotopes.

From ANSI/ANS 5.1-1979, the decay heat power is given by the following for a single fissionable isotope:

$$F(t_j, T) = \sum_{i=1}^{23} \frac{\alpha_i}{\Gamma_i} e^{-\Gamma_i t_j}\left(1 - e^{\Gamma_i T}\right) \qquad (3)$$

where the summation is over the 23 pseudo-nuclides, α_i and Γ_i are energy yield fraction and decay constant values from ANSI/ANS 5.1-1979, respectively, T is the operation time (taken to be 10^{13} seconds in the standard), and t_j is the cooling time. Tables 4, 5, and 6 of the standard give decay heat power values for U-235, Pu-239, and U-238, respectively, for 55 cooling times in each table. Thus, there are effectively 55 t_j values for which the standard provides one sigma uncertainty values. [

]^{a,c}

Table RAI-20-1 Fitting Data for κ and σ_κ

a,c

Term	C_i^{κ}	$C_i^{\sigma\kappa}$	L	M	N

Table RAI-20-1 Fitting Data for κ and σ_κ

Term	C_i^κ	$C_i^{\sigma\kappa}$	L	M	N

[a,c

]a,c

Question 21:
(^{235}U, ^{238}U, and ^{239}Pu Decay Heat and Uncertainty Comparison to ANS 5.1-1979)

WCAP-16996-P/WCAP-16996-NP, Volumes I, II and III, Revision 0, Section 9.7, "Decay Heat Uncertainty Evaluation," in discussing the decay heat uncertainty modeling in WCOBRA/TRAC-TF2, refers to Figures 9-26 to 9-28 for comparison of "predicted decay heat with uncertainties to the standard decay heat plus 2σ uncertainties" for cooling times from 1 s to 10^9 s. Figure 9-26 shows the decay heat for ^{235}U, Figure 9-27 exhibits the decay heat for ^{239}Pu, and Figure 9-28 plots the decay heat for ^{238}U as functions of cooling time after shutdown and each plot identifies three data sets. The first data set is labeled "DH Standard" and the second data set is labeled "DH Standard + 2 Sigma" in all three plots. The third data set is labeled as "DH Fitted" in Figure 9-26 and as "DH Calculated" in Figures 9-27 and 9-28.

Please clarify and address, as needed, the following comments related to Section 9.7 and Figures 9-26 to 9-28.

(1) It is believed that the units for decay heat on the Y-axis in each figure should be "MeV/fission" (MeV/fission=[MeV/s]/[fission/s]). Instead, the decay heat units appear as "MeV/sec/fission".
(2) It appears that that Figure 9-26 exhibits the decay heat function $F_i(t,T)$ for thermal fission of ^{235}U, Figure 9-27 plots $F_i(t,T)$ for thermal fission of ^{239}Pu, and Figure 9-28 shows $F_i(t,T)$ for fast fission of ^{238}U for infinite irradiation time ($T=10^{13}$ s) in all three plots. However, description for the plotted quantities is not provided in Section 9.7.
(3) Only two data sets (curves) are seen in each of the plots. A third data set (curve) is not distinguishable and using symbols to indicate overlapping curves can be used if appropriate.

Please provide updated plots that represent the WCOBRA/TRAC-TF2 decay heat predictions for ^{235}U, ^{239}Pu, and ^{238}U for decay time from 0.1 s to 10^6 s. In each plot, please show the standard decay heat values $F_i(t,\infty)$ for ^{235}U, ^{239}Pu, and ^{238}U as tabulated in ANSI/ANS 5.1-1979 Tables 4, 5, and 6 representing each value by a symbol with a two-sided Y-error bar corresponding to $\pm 2\sigma$ uncertainty using the uncertainty data in the ANSI/ANS 5.1-1979 tables. The uncertainties in both ANSI/ANS 5.1-1979 and ANSI/ANS 5.1-2005 are currently represented in tabular form for the decay heat functions $f_i(t)$ and $F_i(t,\infty)$ and values for intermediate times are obtained by interpolation. The included figure presents the $F_i(t,\infty)$ ANSI/ANS 5.1-1979 Standard decay heat and uncertainty data for ^{235}U, ^{239}Pu, and ^{238}U. In each figure, plot a curve that shows the "nominal" WCOBRA/TRAC-TF2 decay heat prediction as a continuous function of time and then show two additional curves that represent uncertainties predicted by WCOBRA/TRAC-TF2 and representing the decay heat "upper bound" (nominal plus 2σ) and "lower bound" (nominal minus 2σ). Explain how the code predicts the uncertainties for $t < 1$ s as no standard data are provided.

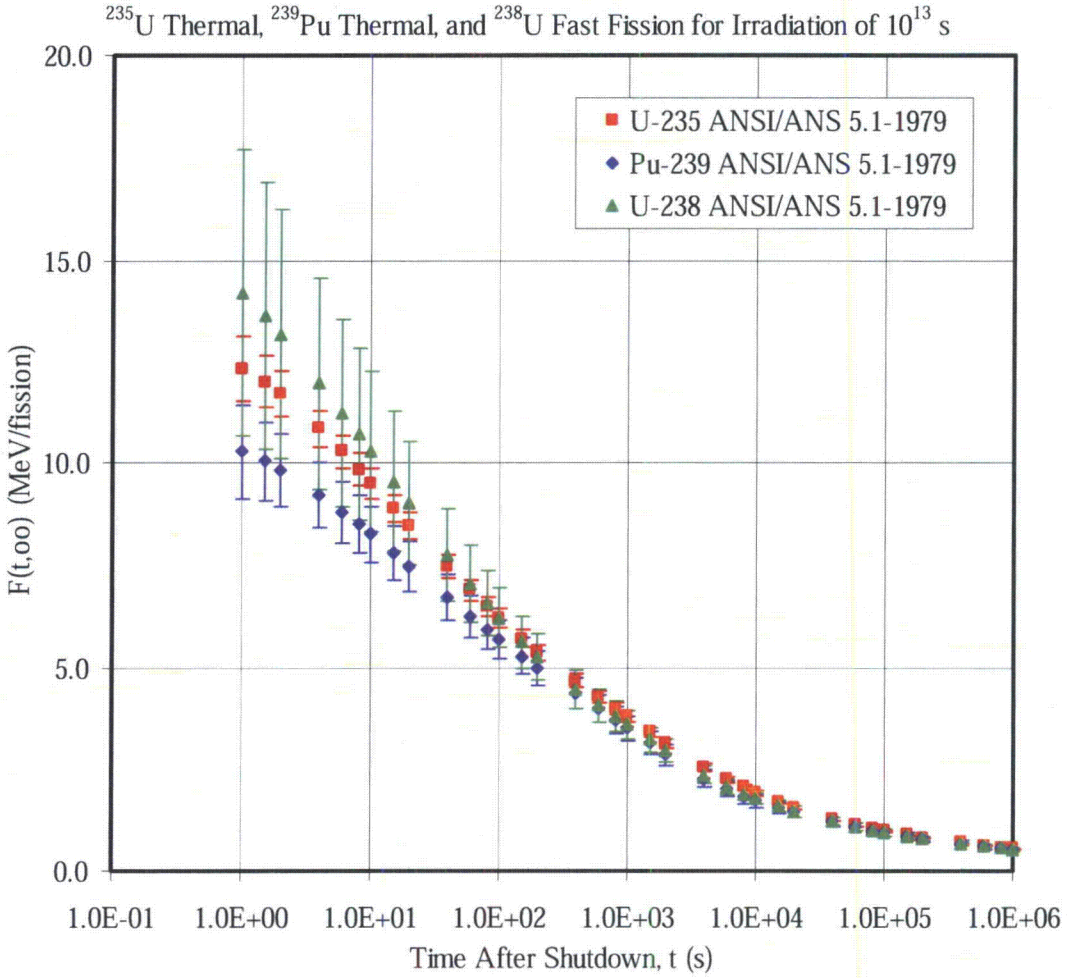

Figure: ANSI/ANS 5.1-1979 Tabular Data for Standard Decay Heat Power and Uncertainty for Thermal Fission of ^{235}U and ^{239}Pu and Fast Fission of ^{238}U for Irradiation of 10^{13} s

Response:

The following responses pertain to the numbered questions/comments in RAI-21:

(1) The units for decay heat power on the Y-axis in Figures 9-26 through 9-28 should be MeV/fission.
(2) Figures 9-26 through 9-28 display the comparison of decay heat power functions $F_i(t,T)$ for thermal fission of ^{235}U, thermal fission of ^{239}Pu, and fast fission of ^{238}U for infinite irradiation time calculated with WCOBRA/TRAC-TF2 and the ANSI/ANS-5.1-1979 standard .
(3) See Figures RAI-21-1 through RAI-21-3 for updated plots with more visible lines.

Figures RAI-21-1 through RAI-21-3 provide curves that represent the nominal WCOBRA/TRAC-TF2 decay heat power predictions as continuous functions of time, as well as two additional curves that represent the decay heat power "upper bound" (nominal plus 2σ) and "lower bound" (nominal minus 2σ) for ^{235}U, ^{239}Pu, and ^{238}U for decay time from 0.1 s to 10^6 s. In addition, each plot includes the standard

decay heat power values $F_i(t,\infty)$ for ^{235}U, ^{239}Pu, and ^{238}U as tabulated in ANSI/ANS 5.1-1979 Tables 4, 5, and 6, representing each value by a symbol with a two-sided Y-error bar corresponding to $\pm 2\sigma$ uncertainty using the uncertainty data in the ANSI/ANS 5.1-1979 tables.

To calculate the decay heat power uncertainty prior to 1 second after shutdown, Equation 4 of the response to RAI Question 20 is used.

It is noted that the WCOBRA/TRAC-TF2 code version used to generate the data presented in Figures RAI-21-1 through RAI-21-3 corrects several errors in the existing configured WCOBRA/TRAC-TF2 code version relevant to this RAI response. The identified WCOBRA/TRAC-TF2 code errors are as follows:

1. The decay group uncertainty factors (in Table 9-14 of WCAP-16996-P) for ^{239}Pu are applied to ^{238}U, and the decay group uncertainty factors for ^{238}U are applied to ^{239}Pu.
2. The decay group uncertainty factor for Group 6 of ^{235}U is erroneously coded as 2.5% instead of 2.25%.
3. The yield fraction directly from fission (α) for Group 19 of ^{239}Pu is erroneously coded as 5.703E-11 instead of 5.730E-11.

Figures RAI-21-4 through RAI-21-6 provide the same curves as RAI-21-1 through RAI-21-3, except that they are produced using a WCOBRA/TRAC-TF2 code version containing the errors described above. By comparing Figures RAI-21-4 through RAI-21-6 to Figures RAI-21-1 through RAI-21-3, the following observations are made:

- Error 2 identified above has a negligible impact based on the WC/T Nominal $\pm 2\sigma$ lines in Figures RAI-21-1 and RAI-21-4 (maximum deviation of less than 0.09%).
- Error 3 identified above has a negligible impact based on the WC/T Nominal lines in Figures RAI-21-2 and RAI-21-5 (maximum deviation of less than 0.07%).
- The WC/T Nominal $\pm 2\sigma$ lines in Figures RAI-21-5 and RAI-21-6 show that Error 1 identified above causes over-prediction of uncertainty in decay power from ^{239}Pu and under-prediction of uncertainty in decay power from ^{238}U. Figures RAI-21-7 and RAI-21-8 compare the normalized 1σ uncertainty factor with and without the errors as a function of burnup and enrichment immediately after shutdown. These curves are calculated taking the fission fractions for each isotope into account. Figure RAI-21-9 shows a comparison of the 5 w/o enrichment curves with and without the errors. From these figures, it is concluded that this error results in an over-prediction of decay heat power uncertainty for fuel rods with burnup greater than about 5000 MWD/MTU and positive sampled uncertainty. For fuel rods with burnup less than 5000 MWD/MTU and positive sampled uncertainty, the under-prediction of decay heat power uncertainty varies from about 0.4% to 0 between about 0 and 5000 MWD/MTU.

[ ] a,c

Figure RAI-21-1 Comparison of Decay Heat Power Predictions for Thermal Fission of U-235 between ANSI/ANS 5.1 – 1979 Decay Heat Standard and WC/T with Errors Corrected

[a,c]

Figure RAI-21-2 Comparison of Decay Heat Power Predictions for Thermal Fission of Pu-239 between ANSI/ANS 5.1 – 1979 Decay Heat Standard and WC/T with Errors Corrected

[a.c]

Figure RAI-21-3 Comparison of Decay Heat Power Predictions for Fast Fission of U-238 between ANSI/ANS 5.1 - 1979 Decay Heat Standard and WC/T with Errors Corrected

[a,c

]

Figure RAI-21-4 Comparison of Decay Heat Power Predictions for Thermal Fission of U-235 between ANSI/ANS 5.1 – 1979 Decay Heat Standard and WC/T with Errors

[a,c

]

Figure RAI-21-5 Comparison of Decay Heat Power Predictions for Thermal Fission of Pu-239 between ANSI/ANS 5.1 – 1979 Decay Heat Standard and WC/T with Errors

a,c

Figure RAI-21-6 Comparison of Decay Heat Power Predictions for Fast Fission of U-238 between ANSI/ANS 5.1 – 1979 Decay Heat Standard and WC/T with Errors

[ ]a,c

Figure RAI-21-7 Comparison of Normalized 1σ Uncertainty Factor as a Function of Burnup and Enrichment with Errors Corrected

[a,c

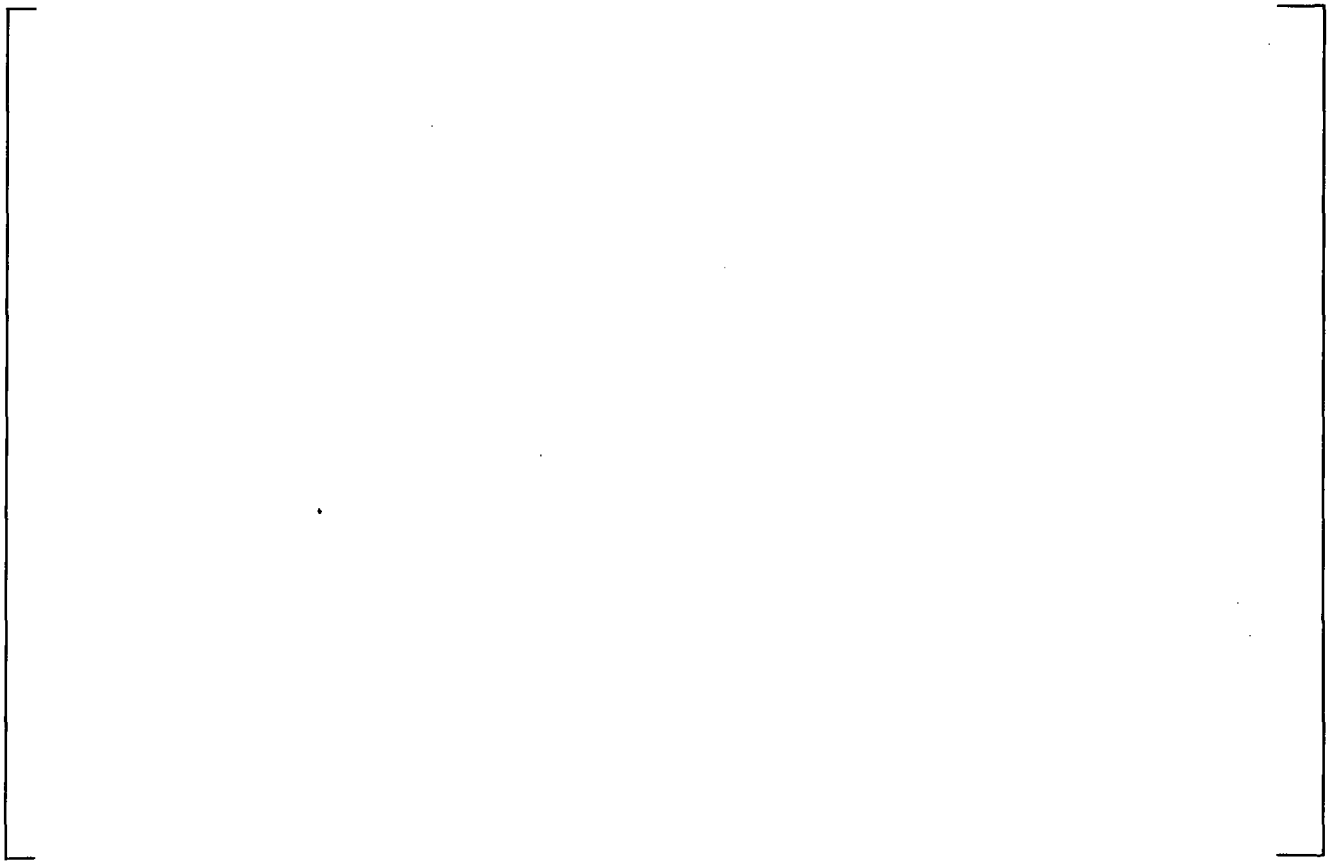

]

Figure RAI-21-8 Comparison of Normalized 1σ Uncertainty Factor as a Function of Burnup and Enrichment with Errors

a,c

Figure RAI-21-9 Comparison of Normalized 1σ Uncertainty Factor for 5 w/o Enrichment as a Function of Burnup

Question 22:
(^{235}U, ^{238}U, and ^{239}Pu Decay Heat Uncertainty Comparison to ANS 5.1-1979)

The determination of decay heat uncertainties is an important area and the modeling of decay heat uncertainty in WCOBRA/TRAC-TF2 is discussed in WCAP-16996-P/WCAP-16996-NP, Volumes I, II and III, Revision 0, Section 9.7, "Decay Heat Uncertainty Evaluation." WCOBRA/TRAC-TF2 models decay heat uncertainty through the use of pseudo-isotope energy yield augmentation factors generated using a least squares fit to the uncertainty data provided in ANSI/ANS 5.1-1979. The section refers to Figures 9-23 to 9-25 stating that they "illustrate the fit deviation in both energy and decay heat versus cooling time." According to the figure captions, the plots represent "percent fit deviations" for ANSI/ANS 5.1-1979 plus 2σ for ^{235}U, ^{239}Pu, and ^{238}U.

It is seen from Figures 9-23 to 9-25 that the plotted discrepancies exhibit most pronounced deviation during the first 100 s of cooling time. At the same time, approximately 25% of the residual decay energy is released in the first 10 s after the fission process ends and about 50% is released by 100 s after fission (see I. Gauld, "Validation of ORIGEN-S Decay Heat Predictions for LOCA Analysis," PHYSOR-2006, ANS Topical Meeting on Reactor Physics, Vancouver, BC, Canada, September 10-14, 2006).

Please explain how the quantity labeled "Deviation" and shown along the vertical Y-axis in Figures 9-23 to 9-25 for cooling time from 10^{-1} s to 10^{9} s was computed and define the parameters "energy" and "decay heat" for which the results were plotted. Please provide updated plots that compare the WCOBRA/TRAC-TF2 uncertainty predictions for ^{235}U, ^{239}Pu, and ^{238}U for cooling time from 0.1 s to 10^{6} s. In each plot, please show the uncertainty presented as $1+2\sigma$ and computed using the tabulated σ uncertainty percent values provided in ANSI/ANS 5.1-1979 Tables 4, 5, and 6. The included figure presents the ANSI/ANS 5.1-1979 Standard decay heat uncertainty data for ^{235}U, ^{239}Pu, and ^{238}U. In each figure, plot a curve that shows the WCOBRA/TRAC-TF2 decay heat uncertainty prediction as a continuous function of time. Explain how the code predicts the uncertainties for $t < 1$ s as no standard uncertainty data are provided. If the WCOBRA/TRAC-TF2 decay heat uncertainty model underestimates any of the ANSI/ANS 5.1-1979 Standard values, a correction factor needs to be implemented to ensure that the code calculates uncertainties that are not less than the standard values.

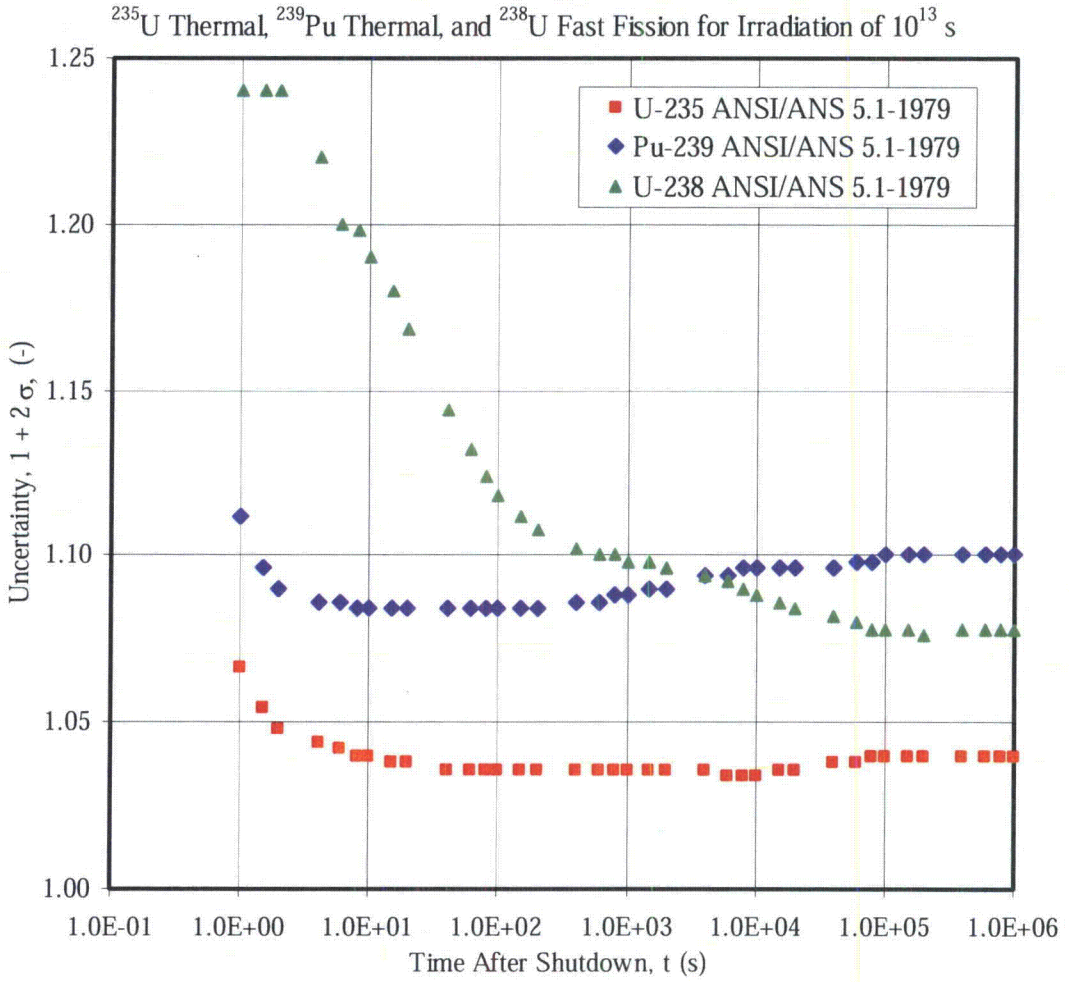

Figure: ANSI/ANS 5.1-1979 Tabular Data for Standard Decay Heat Power Uncertainty for Thermal Fission of ^{235}U and ^{239}Pu and Fast Fission of ^{238}U for Irradiation of 10^{13} s

Response:

The lines designated as decay heat in Figures 9-23 through 9-25 represent the percent deviation between the WCOBRA/TRAC-TF2 decay heat power predictions in Mev/fission and the standard decay heat power values $F_i(t,\infty)$ from ANSI/ANS 5.1-1979 in Mev/fission. The percent deviation is calculated according to Equation (1).

$$\%Dev_{DH} = \frac{DH_{WC/T} - DH_{Standard}}{DH_{Standard}} * 100 \qquad (1)$$

The lines designated as decay energy in Figures 9-23 through 9-25 represent the percent deviation in decay power integrated over the cooling time between WCOBRA/TRAC-TF2 and the standard decay heat power values $F_i(t,\infty)$ from ANSI/ANS 5.1-1979. Specifically, to calculate the decay energy between any two cooling times, t_1 and t_2:

$$DE(t_2 - t_1) = \int_{t_1}^{t_2} DH(t)\, dt \qquad (2)$$

Equation (2) produces decay energy results with units of MeV/fission/sec. [

]^{a,c}

Finally, to obtain the percent deviation given in Figures 9-23 through 9-25, Equations (1) and (7) are used at each time step for decay heat power and decay energy, respectively.

$$\%Dev_{DE} = \frac{DE_{WC/T} - DE_{Standard}}{DE_{Standard}} * 100 \qquad (7)$$

Figures RAI-22-1 through RAI-22-3 show the nominal WCOBRA/TRAC-TF2 decay heat power predictions plus 2σ uncertainty as continuous functions of time for ^{235}U, ^{239}Pu, and ^{238}U, presented normalized to the nominal values. In addition, the ANSI/ANS 5.1-1979 standard decay heat power uncertainty data for ^{235}U, ^{239}Pu, and ^{238}U is presented in the same format.

To calculate the decay heat power uncertainty prior to 1 second after shutdown, Equation (4) of the response to Draft RAI number 20 is used.

[

]^{a,c}

As discussed in the RAI-21 and RAI-27 responses, ^{238}U contributes less decay heat than ^{235}U and ^{239}Pu. As a result, it is judged that the [

]^{a,c}

Based on the decay heat discussion in Section 2.3.2.1 of WCAP-16996-P Revision 0, decay heat is [ ]^{a,c}

Additionally, at about 10 seconds, the decay energy deviations for each isotope in Figures 9-23 through 9-25 of WCAP-16996-P Revision 0 are positive, which indicates that the total decay energy is over-predicted. The decay energy remains over-predicted until about 400 seconds for ^{235}U, and past 1000 seconds for ^{238}U and ^{239}Pu. [

]^{a,c}

It is noted that the WCOBRA/TRAC-TF2 code version used to generate the data presented in Figures RAI-22-1 through RAI-22-3 is the same as that used to generate Figures RAI-21-1 through RAI-21-3 and thus has the same error corrections described in the response to RAI 21.

[a,c]

Figure RAI-22-1 Comparison of Decay Heat Power Uncertainty Predictions for Thermal Fission of U-235 between ANSI/ANS 5.1 – 1979 Decay Heat Standard and WC/T

[a,c

]

Figure RAI-22-2 Comparison of Decay Heat Power Uncertainty Predictions for Thermal Fission of Pu-239 between ANSI/ANS 5.1 – 1979 Decay Heat Standard and WC/T

[a,c]

Figure RAI-22-3 Comparison of Decay Heat Power Uncertainty Predictions for Fast Fission of U-238 between ANSI/ANS 5.1 – 1979 Decay Heat Standard and WC/T

Question 23: Burnup Limit in Assessing Kinetics Parameters

WCAP-16996-P/WCAP-16996-NP, Volumes I, II and III, Revision 0, Section 9, "WCOBRA/TRAC-TF2 Reactor Kinetics and Decay Heat Models," includes Figures 9-1 through 9-3, Figures 9-5 through 9-15, and Figures 9-32 through 9-34 that illustrate the dependence of various important physical parameters on the fuel burnup. With regard to neutron kinetics, WCAP-16996-P/ WCAP-16996-NP, Volumes I, II and III, Revision 0, Section 9.3, "Fission Heat," states that WCOBRA/TRAC-TF2 explicitly models the burnup and initial enrichment dependence of kinetics data. Such data, generated for typical Westinghouse fuel lattice designs, are presented in Figures 9-5 through 9-14.

In all identified figures, the burnup range is limited to 60 MWD/MTU. Please explain if the application of the FSLOCA™ methodology is limited by this burnup level. If this is not the case, please show revised plots that cover the entire expected range of fuel burnup levels.

Response:

Westinghouse fuel is currently licensed to a peak rod burnup of 62,000 MWD/MTU. [

]^{a,c} In general, the fuel with the highest burnup is modeled on the core periphery. In typical core loading patterns, high burnup fuel is placed on the core periphery to improve fuel economy. [

]^{a,c} Should Westinghouse seek approval to increase the peak rod burnup beyond 62,000 MWD/MTU at some future time, the adequacy of the fitting parameters and the 0-60,000 MWD/MTU burnup range will be revisited.

Question 24: Editorial

WCAP-16996-P/WCAP-16996-NP, Volumes I, II and III, Revision 0, Section 9.10, "Generalized Energy Deposition Model (GEDM) Validation," refers to Table 9-19 for a comparison [ ] Table 9-19 is not found in WCAP-16996-P Revision 0. It is believed that the referenced table should be Table 9-18 instead of Table 9-19. Please clarify and correct accordingly.

WCAP-16996-P/WCAP-16996-NP, Volumes I, II and III, Revision 0, Subsection 9.9.2, "WCOBRA/TRAC-TF2 Fission Energy Accounting," refers to Table 9-18 with regard to the prompt fission energy release, radiative capture release, and average fission neutron energy utilized in the evaluation of the composite prompt energy release per fission. It is believed that the referenced table should be Table 9-17 instead of Table 9-18. Please clarify and correct accordingly.

WCAP-16996-P/ WCAP-16996-NP, Volumes I, II and III, Revision 0, Subsection 9.9.1, "Actinide Decay Power," with regard to physical data for [ ]^{a,c} used in calculations performed to evaluate the impact of the total actinide heat source. It is believed that the referenced table should be Table 9-16 instead of Table 9-17. Please clarify and correct accordingly.

Response:

Westinghouse agrees that the items noted in RAI #24 are incorrect. Revisions to reflect the correct cross-references will be made as part of the overall topical report revision.

Question 25: Utilized Codes

WCAP-16996-P/WCAP-16996-NP, Volumes I, II and III, Revision 0, Section 9.2, "Decay Heat Source, explains that WCOBRA/TRAC-TF2 solves the time-dependent decay activity differential equation accounting for ^{235}U and ^{239}Pu thermal fission as well as for ^{238}U fast fission. The energy yield constants are weighted by the appropriate fission rate fractions as a function of initial enrichment and burnup within WCOBRA/TRAC-TF2. It is explained that the fission rate weighting was obtained from detailed physics evaluations of PWR fuel lattice designs and the results from these evaluations are presented in Figure 9-1 for ^{235}U thermal fission and in Figures 9-2 and 9-3 for ^{239}Pu thermal fission and ^{238}U fast fission weightings, respectively. Thus, WCOBRA/TRAC-TF2 solves for the composite decay heat of the reactor of interest using the fission rate fractions derived from specific physics calculations for the fuel lattice design. Please identify the codes used to perform these calculations, explain if they have been approved by NRC, and provide appropriate references.

WCAP-16996-P/WCAP-16996-NP, Volumes I, II and III, Revision 0, Section 9.3, "Fission Heat," states that a series of detailed space/energy calculations have been performed for a typical fresh assembly to quantitatively evaluate fission rate per unit neutron density for water densities that occur during a LOCA transient. Figure 9-4 shows the calculated coolant density dependence of the macroscopic cross section. Please identify the codes used to perform these calculations, explain if they have been approved by NRC, and provide appropriate references. In addition, please identify and explain the values for the physical parameters "KSF," "NSF," and "SIGA" that are used to indentify each of the three curves shown in Figure 9-4. Which of the results was used to model the fission frequency in WCOBRA/TRAC-TF2?

WCAP-16996-P/WCAP-16996-NP, Volumes I, II and III, Revision 0, Subsection 9.6.2, "GEDM," explains that the DOT code was used as the dimensional particle transport code for the examples presented in this report. Please explain if this code has been approved by NRC and provide appropriate references.

WCAP-16996-P/WCAP-16996-NP, Volumes I, II and III, Revision 0, Subsection 9.9.1, "Actinide Decay Power," explains that detailed calculations have been performed to evaluate the impact of the total actinide heat source. Please identify the codes used to perform these calculations, explain if they have been approved by NRC, and provide appropriate references.

Response:

The fission rate fractions and coolant density dependence of the macroscopic cross sections were generated using a Westinghouse unit cell depletion program (ARK) which evolved from the codes LEOPARD and CINDER and additionally included a higher order matrix exponential method option for calculation of depletion isotopics. The references for these codes are provided below:

R. F. Barry, "LEOPARD - A Spectrum Dependent Non-Spatial Depletion Code for the IBM-7094," WCAP-3269-26, Westinghouse Electric Corporation (September, 1963).

T. R. England, "CINDER - A One-Point Depletion and Fission Product Program," WAPD-TM-334, Westinghouse Electric Corporation Bettis Atomic Power Laboratory (August, 1962).

LEOPARD and CINDER have not been formally generically approved, but their use has been documented and licensed in FSAR's dating back to the 1970's.

The values for the physical parameters "KSF," "NSF," and "SIGA" that are used to indentify each of the three curves shown in Figure 9-4 are simply the normalization factors for each of the curves. Each curve

is normalized to a value of 1.0 at a water density of 0.7 gm/cm^3. So, for example, the Σ_A curve ("SIGA") is normalized using the factor [ ]^{a,c} which is the value of Σ_A in units of cm^{-1} at 0.7 gm/cm^3.

The fission frequency, which is $v\kappa\Sigma_F$, [ ]^{a,c} using the specific curves given in Figure 9-4. The density dependence of the fission frequency, [ ]^{a,c} the formulation given in Table 9-5. This formulation accounts for the density dependence of the $\kappa\Sigma_F$ portion of the fission frequency. The average neutron velocity, v, increases as density decreases. So, the density dependence of $v\kappa\Sigma_F$ is not the same as the density dependence of $\kappa\Sigma_F$.

The DOT code, which was the basis for the DORT code, is a radiation transport code that employs a standard industry method. Use of DORT has been approved by the NRC in the following topical report:

> Anderson, S. L., "Benchmark Testing of the FERRET Code for Least Squares Evaluation of Light Water Reactor Dosimetry," WCAP-16083-NP-A, Westinghouse Electric Company, LLC, May 2006.

In WCAP-16083-NP-A, DORT has the following reference:

> RSICC Computer Code Collection CCC-650, "DOORS 3.1, One- Two- and Three-Dimensional Discrete Ordinates Neutron/Photon Transport Code System," Radiation Safety Information Computational Center, Oak Ridge National Laboratory (ORNL), August 1996.

The actinide decay power heat source was determined using actinide number densities generated using the above-mentioned Westinghouse unit cell depletion program with the matrix exponential method employed.

Question 26: Actinides Decay Heat Power

In treating actinide decay heat power, ANSI/ANS 5.1 explicitly considers only decay heat power from ^{239}U and ^{239}Np. These two actinide isotopes are the dominant actinide decay heat for cooling times for which the standard is routinely applied to calculate decay heat for thermal-hydraulic safety system analyses. This limitation of the standard necessitates consideration of its augmentation with actinide values obtained from other calculations as actinide contribution, with ^{239}U and ^{239}Np excluded, increases from approximately 1 percent of the fission product decay heat power after 1 s up to approximately 10 percent after 10^5 s following shutdown (I.C. Gauld et al., "Proposed Revision of the Decay Heat Standard ANSI/ANS-5.1-2005," ORNL Publication No. 24753, October 2011). WCAP-16996-P/WCAP-16996-NP, Volumes I, II and III, Revision 0, Subsection 9.9.1, "Actinide Decay Power," presents results from detailed calculations performed to evaluate the impact of the total actinide heat source. As seen from Figures 9-32 and 9-33 [

]^{a,c} Please present the analysis results that quantify the impact of [

]^{a,c} Identify the assumptions applied in this analysis and show the results for the predicted actinide power for both cases [

]^{a,c} Illustrate the impact from major parameters over their entire range of interest for decay heat predication.

Response:

The actinide decay heat power at any particular core position is dependent upon the power density history of that core position. The half-lives of ^{239}U and ^{239}Np are 0.39 hr and 56.4 hr, respectively. Because the half-life of ^{239}U is relatively short, decay heat due to ^{239}U will reach its equilibrium value within a few hours after a step change in the local power density. This is not the case for ^{239}Np. For ^{239}Np, the decay heat only approaches its equilibrium value after several days following a step change in local power density. The decay heat from ^{239}Np represents about 47% of the total decay heat from both isotopes in equilibrium. Consequently, after any change in local power density, the total actinide decay heat from both isotopes will lag the equilibrium actinide decay heat primarily because of the lag in the contribution from ^{239}Np.

The kinds of peak local power densities that are limiting from a LOCA perspective are caused by non-equilibrium operation of the core, e.g., due to load follow. Changes in the core power level and core power distribution cause changes in the core xenon distribution. The result, in the absence of tight reactor control, is a dynamic reactor response which can lead to highly peaked power shapes. Such power shapes, however, occur over shorter time scales than the half-life of ^{239}Np. The time scale for load follow is 24 hours. Therefore, a core performing continuous load follow will cycle between peak power densities over a 24 hour period. The time scale for xenon changes is determined by the half-life of ^{135}Xe, which is about 9 hours. Consequently, the power shapes and local power densities that are limiting from a LOCA perspective are not stable and will naturally exist for only a few hours before other dynamic effects, such as xenon destruction, decay, or production, cause the power distribution to change.

To quantify the decay heat effects of non-equilibrium operation, it is necessary to make assumptions about the power density history. In the discussion below, the response of the actinide decay heat to a step change in power density and to power density changes typical of daily load follow will be described. Of

course, the number of possible power density histories is infinite. The examples provided serve to illustrate a range of possible decay heat responses relative to the assumption of equilibrium actinide decay heat.

To quantify the temporal behavior of the ^{239}U and ^{239}Np decay heat for a power density history, it is useful to solve the differential equations (9-12) and (9-13) given in Section 9.4 of WCAP-16996-P Revision 0. These equations are repeated below as equations (1) and (2):

$$\frac{dP_u}{dt} = \bar{R}\alpha_u[v\Sigma_F n(t)] - \lambda_u P_u(t) \quad (1)$$

$$\frac{dP_n}{dt} = \frac{\lambda_u P_u(t)\alpha_n}{\alpha_u} - \lambda_n P_n(t) \quad (2)$$

where:

$v\Sigma_F n(t)$ = time-dependent fission rate (proportional to power density),
λ_u = ^{239}U decay constant = 4.91E-4 sec^{-1},
λ_n = ^{239}Np decay constant = 3.41E-6 sec^{-1},
$\bar{R}(BU, \varepsilon)$ = ^{238}U capture-to-fission ratio, function of initial enrichment ε, and burnup (BU),
$P_u(t)$ = time dependent decay power due to ^{239}U decay,
q_u = energy release per ^{239}U decay = 0.474 MeV,
$P_n(t)$ = time dependent decay power due to ^{239}Np decay,
q_n = energy release per ^{239}Np decay = 0.419 MeV,
$\alpha_u = q_u\lambda_u$ decay power yield per capture (MeV/sec/capture) for ^{239}U, and
$\alpha_n = q_n\lambda_n$ decay power yield per capture (MeV/sec/capture) for ^{239}Np.

[

]^{a,c}

[ ] a,c (3)

(4)

Equations (1) and (2) can be readily solved if one assumes a constant fission rate over a short time step Δt. If we specify the constant fission rate as Q, the solutions for the time dependent decay powers over the time step are given by the following expressions:

[ ] a,c (5)

(6)

[

]a,c

Suppose a step change in power density is assumed from a relative power density of 1.0 to 1.4, i.e., Q in the above expression increases instantaneously from a steady state value of 1.0 to 1.4 at time 0 and then remains at this value. (This is analogous to the local F_Q*Power value increasing, e.g., from a steady state value of 1.8 to 2.52 since 2.52/1.8 = 1.4). Figure RAI-26-1 shows the resulting time dependent decay heat values for ^{239}U and ^{239}Np and for the sum of both. [
]a,c are also given. This figure assumes an $\overline{R}$ value (^{238}U capture/fission ratio) of 0.6, corresponding to low burnup, high enrichment fuel. As will be shown later, the value for is not important to the relative difference between [

]a,c

[

]a,c

The above step change is not a realistic case since such a large increase in local power density above the natural steady-state value cannot be maintained for such an extended period, i.e., days. A more realistic, but still conservative, assumption is to assume a periodic variation in power density such as would be experienced for continuous daily load follow. Figure RAI-26-2 shows four power density (or fission rate) profiles (i.e., Q(t) profiles) that will be examined to determine how the maximum decay heat experienced during the load follow day compares with the decay heat value resulting from the [
]a,c

These power profiles correspond to a 12-3-6-3 load follow scheme, i.e., 12 hours at the peak power density followed by a 3 hour ramp to the minimum power density, followed by 6 hours at the minimum power density, followed by 3 hour ramp back to the peak power density. This profile mimics a typical load follow schedule. It is conservatively assumed that the peak Q value remains constant for 12 hours during the load follow day. This is equivalent to assuming that the peak F_Q peaking factor (the peak to average power density) in the core is maintained at a constant value while the core is at full power. (Effectively, one can view the power density profiles as having a constant F_Q value throughout but with core power level cycling over a 24 hour period. The power density and the fission rate are proportional to F_Q*Power.) This assumption is conservative since it would be very difficult, due to xenon feedback, to maintain the local power density at a large non-equilibrium peak value for 12 hours. Also, this kind of operation would not be consistent with recommended axial power distribution control strategies. For present purposes, however, [

]a,c

Equations (5) and (6) were used to determine the time dependent decay heat values for an equilibrium load follow cycle. To achieve equilibrium, the load follow decay heat cycle was repeated until equilibrium was achieved. A time step size of 1 minute was used. This time step is very small relative to the time constants for both ^{239}U and ^{239}Np and, thus, will generate accurate results. A predictor-corrector scheme was also used to minimize any error due to the assumption of a constant Q value over the small

time step. [

]^{a,c}

Figure RAI-26-3 show the time dependent decay heat results for the 1.0-0.50-1.0 Q(t) profile. The maximum decay heat for the load follow cycle occurs at 12 hours, the time at which Q begins to decrease. This is due to the decrease in the decay heat contribution from ^{239}U that begins after hour 12. During the equilibrium cycle, the maximum decay heat value reached 0.492 MeV/fission. [

]^{a,c}

All of the profiles produce results that are qualitatively similar to Figure RAI-26-3. However, the profiles with larger differences between the maximum and minimum Q values also produce larger decay heat differences [ ]^{a,c} Table RAI-26-1 compares the maximum decay heat for all four of the Q(t) profiles. Note that the range of the ratio of the [

]^{a,c} In actual operation, power profiles with large differences between the maximum and minimum power densities will tend to be limiting from a LOCA standpoint since these profiles represent the largest departure from the equilibrium state.

The maximum Q value and power profile are the major parameters affecting the maximum decay heat value and the [

]^{a,c} The other variable that can affect the maximum decay heat is $\overline{R}$. Table RAI-26-2 gives decay heat values for a range of $\overline{R}$ values. The 1.0-0.50-1.0 profile was assumed for this table. As the table shows, a higher $\overline{R}$ increases the decay heat (as expected since more atoms of ^{239}U and ^{239}Np are produced), but the [

]^{a,c}

Table RAI-26-1
Transient and Maximum Equilibrium Actinide Decay Heat (MeV/fission)
for Four Power Density Profiles

[ ] a,c

Note: These decay heat values assume an $\bar{R}$ value of 0.6.

Table RAI-26-2
Transient and Maximum Equilibrium Actinide Decay Heat (MeV/fission)
for a 1.0-0.50-1.0 Power Density Profile and Various $\bar{R}$ Values

[ ] a,c

Figure RAI-26-1 Relative Decay Heat for ^{239}U an d^{239}Np for a Step Change in Relative Power Density from 1.0 to 1.4

a,c

Note: Equilibrium values are for a Q of 1.4

Figure RAI-26-2 Q Profiles used for Study of 239U and 239Np Transient Decay Heat

[] a,c

Note: Q is the relative local power density or fission rate where a Q of 1 corresponds to the maximum power density or fission rate over the cycle. Absolute power density or fission rate values can be determined by multiplying the profile by the peak power density or peak fission rate over the cycle.

Figure RAI-26-3 Relative Total Decay Heat (MeV/Fission) for ^{239}U an d^{239}Np for a Power Density Profile of 1.0-0.50-1.0

[ ] a,c

Question 27: Decay Heat in Demonstration Plant Analyses

WCAP-16996-P/WCAP-16996-NP, Volumes I, II and III, Revision 0 Section 9, "WCOBRA/TRAC-TF2 Reactor Kinetics and Decay Heat Models," describes the models for heat sources from fission heat, fission product decay heat, and actinide decay heat. However, the section does not show a calculated reactor power curve used in any of the analyses discussed in WCAP-16996-P Revision 0.

For the demonstration Westinghouse plant (V. C. Summer) examined in WCAP-16996-P/WCAP-16996-NP, Volumes I, II and III, Revision 0, Section 31, "Full Spectrum LOCA Demonstration Analysis," please present graphs that show the WCOBRA/TRAC-TF2 predicted total residual power relative to the operating power (total reactor power or local power as appropriate) for the Region I and Region II limiting cases (Run 059 and Run 119). Use logarithmic scales for both the X-axis showing time after shutdown or break occurrence from 0.1 s to 10^6 s and for the Y-axis showing relative power from 10^{-3} to 10^0. In each plot, please show with separate curves the residual fission power from the point kinetics model, the individual decay power contributions accounting for fission product decay power, actinide decay power, and decay power due to neutron capture by fission products during irradiation using the ANSI/ANS 5.1-1979 decay heat model, and the resulting total residual power. Present the "nominal" WCOBRA/TRAC-TF2 decay heat curve along with the upper (nominal plus 2σ) and lower (nominal minus 2σ) bounds in the plots. Please include two tables that document all utilized input parameters to the applied WCOBRA/TRAC-TF2 models to compute the contributing residual powers for both runs as plotted in the presented graphs (e.g., energy per fission). For each appropriate input parameter, please show its identifier, units, numerical or logical value, and the way in which the input value was determined. In the same manner, please document also all relevant uncertainty factors applied for both runs. Please explain if suggestions contained in NRC Information Notice 96-39, "Estimates of Decay Heat Using ANS 5.1 Decay Heat Standard May Vary Significantly," dated July 5, 1996, are of relevance when determining any ANSI/ANS 5.1-1979 Standard input model parameters for WCOBRA/TRAC-TF2.

Response:

1.0 Description of Figures

Figure RAI-27-1 presents the total residual power, as well as the individual contributions from the point kinetics model, thermal fission of ^{235}U, thermal fission of ^{239}Pu, fast fission of ^{238}U, actinide decay power, and power production due to neutron capture for the limiting case (Run 59) of Region I in the Westinghouse demonstration plant calculations. These curves are all normalized to initial core power, and they are all calculated using the sampled decay heat power uncertainty value from the demonstration plant analysis.

Figure RAI-27-2 presents the total residual power for Region I, Run 59, normalized to initial core power. The Actual Power curve represents the power calculated using the sampled decay heat power uncertainty value from the demonstration plant analysis. The Nominal Power curve represents the power calculated using no decay heat power uncertainty, and the Nominal $\pm 2\sigma$ curves represent the power modeling nominal $\pm 2\sigma$ decay heat power uncertainty.

Figures RAI-27-3 through RAI-27-5 present power generated by thermal fission of ^{235}U, thermal fission of ^{239}Pu, and fast fission of ^{238}U, respectively, for Region I, Run 59. The curves are all normalized to initial core power. The Actual Power curves represent the power calculated using the sampled decay heat power uncertainty value from the demonstration plant analysis. The Nominal Power curves represent the power calculated using no uncertainty, and the Nominal $\pm 2\sigma$ curves represent the power modeling nominal $\pm 2\sigma$ uncertainty.

Figures RAI-27-6 through RAI-27-8 present the power calculated with the point kinetics model, the actinide power, and power production due to neutron capture, respectively, for Region I, Run 59. The curves are all normalized to initial core power. The Actual Power curves represent the power calculated using the sampled decay heat power uncertainty value from the demonstration plant analysis. The Nominal Power curves represent the power calculated using no uncertainty, and the Nominal ± 2σ curves represent the power modeling nominal ± 2σ uncertainty.

The decay heat power uncertainty sampled for Region I, Run 59 is [ ]^{a,c} Therefore, it is expected that the Actual Power curves in Figures RAI-27-2 through RAI-27-5 show [ ]^{a,c} From Figure RAI-27-2, it can be seen that the initial deviation between the Actual Power and the Nominal Power is very small; however, as the fission power becomes less dominant around 100 seconds, the deviation due to decay heat power uncertainty begins to become more pronounced as decay heat power begins to make up more of the total power. It is shown in Figures RAI-27-6 and RAI-27-7 that decay power uncertainties cause negligible changes to the fission power and actinide power. [

]^{a,c}

Figure RAI-27-9 presents the total residual power, as well as the individual contributions from the point kinetics model, thermal fission of ^{235}U, thermal fission of ^{239}Pu, fast fission of ^{238}U, actinide decay power, and power production due to neutron capture for the limiting case (Run 119) of Region II in the Westinghouse demonstration plant calculations. These curves are all normalized to initial core power, and they are all calculated using the sampled decay heat power uncertainty value from the demonstration plant analysis.

Figure RAI-27-10 presents the total residual power for Region II, Run 119, normalized to initial core power. The Actual Power curve represents the power calculated using the sampled decay heat power uncertainty value from the demonstration plant analysis. The Nominal Power curve represents the power calculated using no decay heat power uncertainty, and the Nominal ± 2σ curves represent the power modeling nominal ± 2σ decay heat power uncertainty.

Figures RAI-27-11 through RAI-27-13 present power generated by thermal fission of ^{235}U, thermal fission of ^{239}Pu, and fast fission of ^{238}U, respectively, for Region II, Run 119. The curves are all normalized to initial core power. The Actual Power curves represent the power calculated using the sampled decay heat power uncertainty value from the demonstration plant analysis. The Nominal Power curves represent the power calculated using no uncertainty, and the Nominal ± 2σ curves represent the power modeling nominal ± 2σ uncertainty.

Figures RAI-27-14 through RAI-27-16 present the power calculated with the point kinetics model, the actinide power, and power production due to neutron capture, respectively, for Region II, Run 119. The curves are all normalized to initial core power. The Actual Power curves represent the power calculated using the sampled decay heat power uncertainty value from the demonstration plant analysis. The Nominal Power curves represent the power calculated using no uncertainty, and the Nominal ± 2σ curves represent the power modeling nominal ± 2σ uncertainty.

The decay heat power uncertainty sampled for Region II, Run 119 is [ ]^{a,c} Therefore, it is expected that the Actual Power curves in Figures RAI-27-10 through RAI-27-13 show [ ]^{a,c} It is shown in Figures RAI-27-6 and RAI-27-7 that decay power uncertainties cause negligible changes to the fission power and actinide power. [

]^{a,c}

2.0 Description of the Calculation of Total Residual Core Power

The total core power is the sum of the fission power calculated by the point kinetics model and the total decay heat power, which is calculated as a sum of the contributions from thermal fissions of ^{235}U and ^{239}Pu, fast fission of ^{238}U, actinide decay, and neutron capture. The input and selected computed parameters related to the fuel rod power calculations for the demonstration plant runs (Run 59 and Run 119) are listed in Tables 1 and 2.

2.1 Calculation of Fission Power with the Point Kinetics Model

The calculation of fission power with the point kinetics model is described in Section 9.3 of WCAP-16996-P, Revision 0. The reactivity in the point kinetics model is coupled with WCOBRA/TRAC-TF2 core thermal hydraulics, and it is also a function of the core-averaged fuel temperature accounting for all of the rods.

2.2 Calculation of Actinide Power

The calculation of actinide decay power is discussed in Sections 9.4 and 9.9.1 of WCAP-16996-P, Revision 0. As discussed in WCAP-16996-P, Revision 0, the capture to fission ratio, $\bar{R}$, is calculated based on the fuel rod burnup and enrichment inputs using Westinghouse correlations developed for its typical PWR fuel lattice design.

2.3 Calculation of Power from Neutron Capture

The calculation of power from neutron capture is described in Section 9.9.3 of WCAP-16996-P, Revision 0. The fissions per initial fissile atom , ψ, is calculated based on correlations developed for typical Westinghouse PWR fuel lattice design, [
]^{a,c}

2.4 Calculation of Decay Heat Power

The calculations of thermal fissions of ^{235}U and ^{239}Pu, and fast fission of ^{238}U are described in Section 9.2 of WCAP-16996-P, Revision 0. The fission fraction for each fissile isotope, w_n, is calculated as a function of rod burnup and enrichment inputs. Additionally, under WCOBRA/TRAC-TF2 user input guidance, the burnups for the hot rod and hot assembly rod are converted to irradiation time (in seconds) and [
]^{a,c} Additionally, the decay heat power uncertainty multipliers in Tables 1 and 2 are used to obtain the decay heat power for each isotope for each WC/T rod, as described in RAI response 21.

3.0 Examination of NRC Information Notice 96-39

NRC Information Notice 96-39 discusses the potential variation in decay heat power predictions using the ANSI/ANS-5.1-1979 Decay Heat Power Standard through user input parameters. In particular, Actinides, R-factor, G-factor, SI, Power history, and Fissile Elements are discussed in the Information Notice. Based on the discussions in Sections 2.2 through 2.4, these parameters are adequately modeled in WCOBRA/TRAC-TF2.

4.0 Known Errors Involved in the Original Calculations

The WCOBRA/TRAC-TF2 code version used to generate the data presented in Figures RAI-27-1 through RAI-27-16 corrects several errors in the existing configured WCOBRA/TRAC-TF2 code version, three of which are discussed in the response to RAI 21. Additionally, the calculation of decay heat power uncertainty in the code is missing the extra term to account for the 1σ uncertainty in the prompt energy per fission (σ_κ/κ), as described in the response to RAI 20. The inclusion of the extra uncertainty associated with the prompt energy per fission results in a slightly more conservative estimation of the total decay heat power uncertainties.

Table 1: Input and Selected Computed Parameters Used to Compute Residual Power for Region I, Run 59

Parameter	Hot Rod (WC/T Rod 1)	Hot Assembly Rod (WC/T Rod 2)	Core Average Rods (WC/T Rods 3 and 4)	Low Power Rod (WC/T Rod 5)

a,c

Table 2: Input and Selected Computed Parameters Used to Compute Residual Power for Region II, Run 119

Parameter	Hot Rod (WC/T Rod 1)	Hot Assembly Rod (WC/T Rod 2)	Core Average Rods (WC/T Rods 3 and 4)	Low Power Rod (WC/T Rod 5)

a,c

[ ] a,c

Figure RAI-27-1 **Total Power and Power Contributors Normalized to the Initial Core Power for Region I, Run 59**

[ ]a,c

Figure RAI-27-2 Total Core Power Normalized to the Initial Core Power for Region I, Run 59

[a,c

]

Figure RAI-27-3 Power Generated by Thermal Fission of U235 Normalized to the Initial Core Power for Region I, Run 59

[a,c]

Figure RAI-27-4 **Power Generated by Thermal Fission of Pu239 Normalized to the Initial Core Power for Region I, Run 59**

[ ]a,c

Figure RAI-27-5 Power Generated by Fast Fission of U238 Normalized to the Initial Core Power for Region I, Run 59

[a,c

]

Figure RAI-27-6 Fission Power Calculated by the Point Kinetics Model Normalized to the Initial Core Power for Region I, Run 59

[a,c

]

Figure RAI-27-7 Actinide Power Normalized to the Initial Core Power for Region I, Run 59

a,c

Figure RAI-27-8 Power Generated by Neutron Capture Normalized to the Initial Core Power for Region I, Run 59

[a,c

]

Figure RAI-27-9 Total Power and Power Contributors Normalized to the Initial Core Power for Region II, Run 119

[a,c]

Figure RAI-27-10 Total Core Power Normalized to the Initial Core Power for Region II, Run 119

[a,c]

Figure RAI-27-11 Power Generated by Thermal Fission of U235 Normalized to the Initial Core Power for Region II, Run 119

[a,c

]

Figure RAI-27-12 Power Generated by Thermal Fission of Pu239 Normalized to the Initial Core Power for Region II, Run 119

[a,c

]

Figure RAI-27-13 Power Generated by Fast Fission of U238 Normalized to the Initial Core Power for Region II, Run 119

[ ] a,c

Figure RAI-27-14 Fission Power Calculated by the Point Kinetics Model Normalized to the Initial Core Power for Region II, Run 119

[a,c

]

Figure RAI-27-15 Actinide Power Normalized to the Initial Core Power for Region II, Run 119

[a,c

]

Figure RAI-27-16 Power Generated by Neutron Capture Normalized to the Initial Core Power for Region II, Run 119

Question 28: Decay Heat Uncertainty Distribution

As described in WCAP-16996-P/WCAP-16996-NP, Volumes I, II and III, Revision 0, Subsection 25.2.1.4, "The Effect of Fuel Burnup on Power Distributions," the time-in-cycle impacts the decay heat as a burnup-dependent parameter. Furthermore, Subsection 29.5.1, "Fuel Rod," explains that the decay heat uncertainties, based on the ANSI/ANS 5.1-1979 standard, "vary with time in cycle as the decay heat contribution from each fissionable isotope changes." Also, Subsection 29.4.1.2, "Reactor Core Power Distributions and Global Uncertainties," states that "uncertainty in decay heat is considered through the application of ANSI/ANS 5.1-1979 Standard (DH, normal distribution)." Table 29-4, "Uncertainty Elements – Power-Related Parameters Defined in Section 29.4.1," describes the decay heat uncertainty distribution as normal and characterizes it with a mean value and a standard deviation σ defined as a function of burnup and enrichment, $\sigma = f$ (burnup, enrichment). Please explain the method of calculating the dependency of the standard deviation σ for the decay heat uncertainty distribution on the fuel burnup and enrichment and present results to illustrate the predicted effect on σ over the entire range of expected burnup levels and enrichments.

Tables 31.3-1a and 31.3-2a in WCAP-16996-P/ WCAP-16996-NP, Volumes I, II and III, Revision 0, Section 31.3, "Analysis of Results for Region I," and Table 31.4-1a in Section 31.4, "Analysis of Results for Region II," include the uncertainty attribute "DECAY HT (-)" along with the values used in the documented runs. If this or any other attributes are related to the decay heat uncertainty characterization, please explain their meaning and relationship to the characteristics defined in WCAP-16996-P/ WCAP-16996-NP, Volumes I, II and III, Revision 0, Table 29-4 to describe the decay heat uncertainty distribution. Also, please explain how "DECAY HT" or any other decay heat related uncertainty attributes are applied in executing the runs and obtaining the WCOBRA/TRAC-TF2 predictions.

Please explain how the ANS 5.1 uncertainties, represented in tabular form in ANSI/ANS 5.1-1979 Tables 1 to 6 for the decay heat functions $f_i(t)$ and $F_i(t, \infty)$, the fission product decay heat power for a pulse and infinite irradiation as a function of time after fission, relate to the decay heat uncertainty distribution parameters and the decay heat related uncertainty attributes considered above. In particular, please explain if dependence of the decay heat uncertainty distribution standard deviation σ or of the decay heat related uncertainty attributes on the cooling time following reactor shutdown is considered in the FSLOCA methodology.

Response:

As discussed in the response to Question 20, the [

]^{a,c}

[a,c]

[

]^{a,c} The effective 1σ uncertainty in the total decay power is determined by the uncertainty in the relative contributions of each of the pseudo-nuclides to the total decay heat. In turn, these contributions will be dependent on burnup and, to a lesser extent, enrichment since the fission fractions for the fissile isotopes are functions of these variables.

To illustrate the dependence of the 1σ uncertainty factor on burnup and enrichment, the total decay heat power with and without uncertainty was calculated for a representative fuel lattice. A 0 second cooling time was assumed; consequently, the decay powers calculated were initial condition values. The decay heat powers were calculated over a range of burnups and enrichments. The ratio of the total decay heat power with and without uncertainty was then determined at each burnup and for each enrichment. Figure RAI-28-1 gives the results.

As this figure shows, the effective 1σ uncertainty factor [

]^{a,c} As the ANS 5.1 Standard shows, the decay power uncertainty for ^{39}Pu is much larger than for ^{235}U. [

]^{a,c}

The decay heat power uncertainty attribute DECAY HT is the variable N_σ in equation 2 of RAI-20. Effectively, the decay heat power uncertainty factor for a given pseudo-nuclide has the following form:

[ ] a,c

The value for DECAY HT (N_σ) is sampled and employed in the above expression to determine the decay heat uncertainty factor for each pseudo-nuclide.

With respect to the decay heat power uncertainties given in the ANS 5.1 tables, these uncertainties were used to determine the values of the A_i decay group 1σ uncertainties for the various pseudo-nuclides such that the decay power with 2σ uncertainty was reproduced over the range of cooling times. The resulting decay heat power fit deviations relative to ANS 5.1 are given in Figures 9-23, 9-24, and 9-25. The fit deviations are quite small, indicating that the A_i factors accurately reproduce the ANS 5.1 decay powers including uncertainty.

[

]^{a,c}

To illustrate this, Figure RAI-28-2 gives the effective decay heat power uncertainty factor versus burnup for 5 w/o fuel over cooling times ranging from 0 to 400 seconds. As ANS 5.1 shows, the decay heat power uncertainties decrease over cooling times of several hundred seconds as the short-lived pseudo-nuclides decay. This behavior is captured in WCOBRA/TRAC-TF2, as Figure RAI-28-2 illustrates.

Figure RAI-28-1 Effective 1σ Decay Heat Power Uncertainty Factor as a Function of Burnup and Enrichment

a,c

Figure RAI-28-2 Effective 1σ Decay Heat Power Uncertainty Factor as a Function of Burnup and Cooling Time

a,c

Question 29: Decay Heat Sampling Approach

WCAP-16996-P/WCAP-16996-NP, Volumes I, II, and III, Revision 0 Subsection 26.2.2, "V. C. Summer Reference Case and Allowable Plant Operating Conditions," explains that the best-estimate methodology establishes a sampling of the distribution of potential uncertainty contributors, which occur due to changes in plant or model variables. The input values for V. C. Summer and Beaver Valley Unit 1 reference cases considered in Section 26, "WCOBRA/TRAC-TF2 Model of Pilot Plants," are divided in three categories: 1) plant physical description, 2) plant initial operating conditions, and 3) accident boundary conditions. Decay heat is not included in the lists of categorized parameters. The parameters in these categories are sampled once for each run in order to initialize the input values needed to analyze the case.

Decay heat generation is a process that occurs in time and as such it differs from the parameters considered in the above identified categories of input parameters. Decay heat measurement data is characterized by experimental uncertainties. Detailed calculations of decay heat bear the uncertainties that originate from errors in the nuclear data and the yields of individual fission products. As a result, uncertainties are inherent to the decay heat generation process and its quantification at any point in time during the cooling period following reactor shutdown. In this regard, please explain the technique, appropriateness, and applicability of the FSLOCA methodology sampling approach in accounting for uncertainties in the decay heat prediction. This RAI question is related to Question 13.

Response:

The decay heat uncertainty is primarily driven by the uncertainties in the number densities of fission product nuclides at the time of the event and the uncertainties in the energy yields resulting from decay of those fission products. The number density uncertainties result from uncertainties in the fission product yields and nuclear data. The uncertainty in the decay heat power as codified in the decay heat standard [1] is an aggregate uncertainty that accounts for the uncertainty in the initial number densities and the uncertainty in the energy yields of the individual pseudo-nuclides. The aggregate uncertainty is a function of cooling time because the energy yields and decay constants of the individual pseudo-nuclides differ from nuclide to nuclide. Consequently, the decay power contribution of any individual fission product nuclide will vary with cooling time, and so its contribution to the total decay power uncertainty will also vary with cooling time.

Since the decay heat uncertainty is driven by uncertainties in the initial concentrations of fission product nuclides, the decay heat uncertainty is related to a physical property of the system at the time of the event. That physical property is the initial number density distribution among the fission product nuclides. By sampling the number of decay heat uncertainty sigmas for each case, the FSLOCA methodology is effectively sampling from a population of different initial number density combinations of fission product nuclides. Since the FSLOCA methodology reproduces the aggregate decay power uncertainties as codified in the standard as a function of cooling time, the methodology will appropriately capture the time-dependent decay power uncertainty that results from uncertainties in the initial fission product number densities.

Detailed descriptions of the nominal value and uncertainty in the decay power calculations are found in the responses to RAIs-13, 21, 22. The examination of each component of decay power for a sample calculation is given in the response to RAI-27.

References:

1. ANSI/ANS-5.1-1979, "American National Standard for Decay Heat Power in Light Water Reactors."